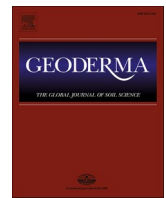# HOKKAIDO UNIVERSITY

Title	Release of essential plant nutrients from manure- and wood-based biochars
Author(s)	Piash, Mahmudul Islam; Iwabuchi, Kazunori; Itoh, Takanori; Uemura, Koki
Citation	Geoderma, 397, 115100 https://doi.org/10.1016/j.geoderma.2021.115100
Issue Date	2021
Doc URL	http://hdl.handle.net/2115/80789
Rights	© 2021 The Authors. Published by Elsevier B.V. This is an open access article under the CC BY license (http://creativecommons.org/licenses/by/4.0/).
Rights(URL)	http://creativecommons.org/licenses/by/4.0/
Type	article
File Information	1-s2.0-S0016706121001804-main.pdf

Instructions for use

Release of essential plant nutrients from manure- and wood-based biochars

Mahmudul Islam Piash [a], Kazunori Iwabuchi [b,*], Takanori Itoh [c], Koki Uemura [a]

[a] Graduate School of Agriculture, Hokkaido University, Kita 9, Nishi 9, Kita-ku, Sapporo, Hokkaido 060-8589, Japan
[b] Research Faculty of Agriculture, Hokkaido University, Kita 9, Nishi 9, Kita-ku, Sapporo, Hokkaido 060-8589, Japan
[c] Tanigurogumi Corporation, Shiobara 1100, Nasushiobara, Tochigi 329-2921, Japan

ARTICLE INFO

ABSTRACT

Several biochars have a considerable amount of essential plant nutrients; however, the release of those nutrients in soil is not well understood. Therefore, in this study, six biochars with varying nutrient contents were produced from Japanese larch (*Larix kaempferi*, JL), dairy manure (DM), and chicken manure (CM) at 300 and 500 °C and incubated in a temperate clay loam soil to investigate their nutrient release dynamics. The available N, P, and K release patterns of the biochars (2% dry-basis) were compared with the recommended fertilizer dose of sweet corn (*Zea mays* convar. *saccharata*) for 120 days. The results indicated that only chicken manure biochars (C/N ratio < 8) have the potential to satisfy plant needs by releasing sufficient N, P, and K. Fourier-transform infrared analysis revealed that N-containing amide dissolution was the major mechanism behind the 49% N release from the CM300 biochar. A higher production temperature (500 °C) diminished most of these amides, resulting in lower N release from CM500 (8.9%). Nitrification-induced reduction of soil pH caused Ca/Mg-P dissolution from manure biochars and enhanced P release. Much of the released phosphates later became unavailable in the soil by aluminosilicate complex formation. DM biochar also released adequate P and K, and production at 500 °C generally performed better than at 300 °C. Effect of coexisting ions on some nutrient release was found, though was statistically nonsignificant. Overall, results revealed that low-temperature (≤500 °C) CM and DM biochars can become comprehensive or complementary sources of plant nutrients, respectively, with some enhanced nutrient-retaining potential, although inherent soil properties may play a significant role.

1. Introduction

Recent increases in global crop production have been mainly achieved by greater inputs of chemical fertilizer (Tilman et al., 2002), and the input is expected to increase further with future food demand. However, the manufacturing process of these synthetic fertilizers is energy-intensive, and mineral stocks for production are also limited. Additionally, the environmental cost of fast-releasing chemicals has been substantial, including water quality degradation, eutrophication, photochemical smog formation, and nitrous oxide emissions (Vitousek et al., 2009). One possible approach to solve these problems is to substitute synthetic fertilizer with renewable and slow-releasing organic fertilizers (Arden-Clarke and Hodges, 1988). Biochar might become a reasonable alternative in this regard, which can efficiently supply soil nutrients and maintain microbial biodiversity for sustainable crop production (Guo et al., 2016; Lehmann and Joseph, 2015).

Carbonization of biomass into biochar has been repeatedly credited for valorizing nutrient elements, improving agronomic benefits, and increasing the residence time of carbon in soil (Lehmann and Joseph, 2015). While most organic fertilizers like manure and mulches undergo fast microbial decomposition, biochar with a large proportion of recalcitrant carbon remains in the soil for a considerably longer period (Duku et al., 2011; Lehmann and Rondon, 2006). Additionally, biochar has the potential to improve some physical, chemical, and biological properties of soil (Guo et al., 2016; Igalavithana et al., 2016). However, most studies so far have mainly focused on the ability of biochars to sequester carbon, remove pollutants, and improve soil physical properties (Kamali et al., 2020). Very few studies have emphasized its nutrient supplying potential, although this could be the key point to encourage marginal farmers for extensive biochar use.

The nutrient supplying potential of biochar is affected by many factors, including the feedstock, production temperature, and physico-chemical properties of the soil itself (Igalavithana et al., 2016; Ok et al., 2018). As reported earlier, most plant-based biochars contain elevated C with lesser quantities of other essential nutrients (Cantrell et al., 2012; Ippolito et al., 2015). Subsequently, negative effects on crop yield have

been reported in some cases (El-Naggar et al., 2019). In contrast, less emphasis has been given to manure-derived biochars that contain significant nutrients (Cantrell et al., 2012), so the release potential of these nutrients is still debatable (Ippolito et al., 2015; Sun et al., 2018b). For instance, biochar made from manures usually has high Ca-containing phosphate minerals, such as hydroxyapatite and octacalcium phosphates, which have very low solubilities (Sun et al., 2018a). Besides, biochars produced at low temperature are reported to have more nitrogen, cation exchange capacity, and surface functional groups, while phosphorus, potassium, and surface area increase with temperature (Song and Guo, 2012; Suliman et al., 2016). These discrepancies in nutrient composition with feedstock and production temperature make it difficult for a particular biochar to act as a comprehensive nutrient source. Consequently, individual studies on N, P, or K release from different biochars have proven inconsistent (Gao et al., 2018; Limwikran et al., 2018).

Moreover, the inherent elemental composition of biochar itself can act as a catalyst for further nutrient release in soil. For example, higher nitrogen content in biochar (low C/N ratio) enhances net mineralization and N release (Chan and Xu, 2009), whereas coexisting ions (NH_4^+, Ca^{2+}, NO_3^-, SO_4^-) can boost P or K release (Subedi et al., 2016; Sun et al., 2018b). To fully understand these interactive processes, more comprehensive studies are required, as the application of biochar intended for improving one nutrient element might affect others. In addition to the elemental composition, release and retention of different nutrients depend on the changes in biochar surface characteristics brought by soil incubation (Ippolito et al., 2015; Mukherjee et al., 2014, 2011). To the best of our knowledge, no previous study has investigated the interactive release of N, P, and K together and their correlation with biochar surface chemistry. Thus, filling these knowledge gaps is essential to understand the differences in biochar nutrient release mechanisms and residual agronomic value for long-term benefits.

In the present research, we hypothesized that greater N content and the presence of coexisting nutrient ions in manure-based biochars will enhance net N mineralization. We further hypothesized that enhanced N mineralization will increase the P and K availability in soil. Therefore, our objectives in this study were 1) to quantify and compare the phytoavailable N, P, and K release from biochars and recommended fertilizer dose for sweet corn, and 2) understand the mechanism of release by investigating biochar surfaces after incubation.

2. Materials and methods

2.1. Collection of soil

Soil was collected from the top 15 cm at the Hokkaido University experimental farm (43° 04′ 24.2″ N, 141° 20′ 13.2″ E), Japan. The site has a mean annual rainfall of 1106 mm and a mean annual air temperature of 8.9 °C. This soil was classified as Japanese brown lowland soil (Haplic Fluvisol) by the Hokkaido Research Organization (2002). According to the National Agriculture and Food Research Organization (NARO), the soil with a yellowish-brown surface layer is the driest land of the alluvial lowlands in Japan. Soil samples were brought to the laboratory, air-dried, and passed through a 2-mm sieve before storing in a polythene bag. The physicochemical properties of the soil are listed in Table S1. Briefly, the particle size determination of the soil revealed that it is a clay loam with 26.27% sand, 37.76% silt, and 35.95% clay. The soil has about 1.91% carbon, 0.026% N, 0.11% P, 0.14% K, a slightly acidic pH with 76.1% base saturation, and a phosphate absorption co-efficient (PAC, an index showing the ability of soil to adsorb and fix phosphates) of 938 (Hokkaido Research Organization, 2012). XRD analysis of the soil (silt and clay) indicated the presence of significant quartz with trace amounts of other minerals including kaolinite, scholzite, ettringite, and leucite.

2.2. Collection of feedstocks and biochar production

Japanese larch (Larix kaempferi, JL), dairy manure (DM), and chicken manure (CM) were used as feedstocks for biochar production. JL was collected as wood shavings. DM was collected from the Hokkaido University dairy farm. CM was collected from a company farm in Hokkaido dedicated to egg production. All the feedstocks were dried in an oven at 105 °C for 24 h before grinding. Powdered raw samples were then passed through a 2-mm sieve. The physicochemical properties of dry feedstocks are presented in Table S2. Biochar was produced in small crucible containers filled with powdered feedstocks with a lid and was placed in a controllable muffle furnace FO810 (Yamato Scientific, Japan) under limited oxygen. The heating rate was set at 10 °C/min, and the production temperature was 300 °C or 500 °C with 1 h of residence time. The biochar samples were allowed to cool in the muffle furnace to room temperature and finally stored in airtight plastic bags, which were named JL300, JL500, DM300, DM500, CM300, and CM500, respectively.

2.3. Incubation experiments

Biochars were incubated in soil by two different setups. To investigate the nutrient release dynamics, glass pots of 150-cm³ volume were used. Treatments comprised control (soil without amendment) and soils treated with recommended chemical fertilizer or six different biochars (2% on a dry-mass basis). The fertilizer treatment received the equivalent amount of the recommended chemical fertilizer dose (12 kg N as NH_4SO_4, 15 kg P_2O_5 as $Ca(H_2PO_4)_2$, and 13 kg K_2O as K_2SO_4 per 100 m² soil for sweet corn production in Hokkaido prefecture (Hokkaido Agriculture Department, 2015). For each nutrient extraction time (0, 7, 14, 21, 28, 42, 56, 88, and 120 days), two replicates for every treatment were prepared. Thus, a total of 144 pots (9 extraction times × 8 treatments × 2 replicates) were used for nutrient release determination. To determine the changes on biochar surfaces and to easily separate biochars from incubated soil, a different setup was used in aluminum pots. These pots received 98 g of dry soil and 2 g of fine (0.5 mm) biochar. The biochar particles were sandwiched between two sheets of nylon mesh (25-μm mesh size) and two equal layers of soil. The biochar samples were spread over the nylon mesh with care to ensure maximum soil interaction and to allow the passage of air, soil solution, and microbial communities. The 6 biochar treatments were replicated twice and prepared separately for collecting biochar samples after 60 days and 120 days of incubation (2 *collection* times × 6 treatments × 2 replicates = 24 pots).

All the pots were subsequently irrigated with distilled water to maintain 60% of the maximum water holding capacity. The pots were then sealed with transparent semi-permeable polythene sheets that allowed air to pass but not water and were kept in a dark incubator at 20 °C for the whole incubation period. The water content was maintained if needed after every 15 days of incubation. Subsamples from particular glass pots were extracted to measure available nutrients, and incubated biochars were separated from aluminum pots, homogenized, and dried before further surface analysis.

2.4. Soil and biochar analysis

2.4.1. Characterization of soil and biochar

The yield (%) of biochar was calculated by the ratio of the mass of biochar by dried biomass, multiplied by 100. The pH of soil and biochar samples were measured using solid to distilled water ratios of 1:2.5 and 1:5, respectively, after 30 min of shaking at 120 rpm. The incubated soil samples were also analyzed for pH using the same procedure as for soil analysis. Cation exchange capacity (CEC) of soil and biochar samples were determined according to Song and Guo (2012). The total C, H, N, and S contents of the soil and biochar samples were determined by a CHN analyzer (CE440) and ion chromatography (Dionex ICS-1600),

respectively. The ash (750 °C) and volatile matter (950 °C) content of biochar samples were determined by following the methods described in ASTM D1762-84 (2013). Total P, K, Ca, Mg, and Na in soil and biochar was determined by ICP-MS (PerkinElmer SCIEX ELAN DRC-e) after digesting with an HNO_3-H_2O_2 system.

2.4.2. Nutrient extraction and determination

The incubated soil samples were extracted with water and 1 M KCl for available nitrate and ammonium, respectively. KCl-extracted samples were further distilled with MgO to remove the interference of K (Jones, 2001). Both nitrate and ammonium ions were determined by the Agilent 7100 Capillary electrophoresis system. To determine the phytoavailable P, K, Ca, and Mg in the treatments, soils were extracted by a Mehlich-3 solution with a ratio of 1:10 (Jones, 2001). Extracts were further digested with HNO_3 before being analyzed with ICP-MS. The nutrient release from biochar was calculated by the following equation:

$$\%\text{nutrient released} = \frac{(\text{Soluble Nutrient}_{\text{in soil+amendment}} - \text{Soluble Nutrient}_{\text{in control}})}{\text{Applied Nutrient}_{\text{in the amendment}}} \times 100$$

Here, Soluble Nutrient$_{\text{in soil+ amendment}}$ indicates the total amount of extractable nutrients in the treatment. To determine the net release from an amendment, nutrient released from the control was subtracted. Applied Nutrient$_{\text{in the amendment}}$ denotes the total amount of N, P, or K supplied by the applied amendment.

2.4.3. FTIR

Fourier transform infrared spectroscopy (FTIR) analysis was performed on a JASCO IRT-3000 N spectrometer equipped with an attenuated total reflectance (ATR) accessory. All pristine and incubated biochar samples were dried at 105 °C, homogenized, ground, and sieved through a 0.5-mm mesh before analysis. Fourier-transform infrared (FTIR) spectra from 128 scans were recorded in the wavenumber range 4000–550 cm^{-1} with a 4-cm^{-1} resolution. The spectrum obtained by the background air in the detection chamber was subtracted from the spectrum of each sample to eliminate the effect of ambient moisture and CO_2. The broadband chemical groups were assigned according to Tipson (1968).

2.4.4. BET specific surface area

The Brunauer-Emmett-Teller (BET) specific surface area (SSA), pore-volume, and average pore size of the soil and biochar samples were analyzed with a BelsorpII mini automated gas sorption system. Before analysis, all biochar samples were outgassed under vacuum at 150 °C for 2 h to eliminate residual moisture before nitrogen gas adsorption. The BET equation was used to calculate the surface area of the biochar.

2.4.5. SEM and EDS

To determine the morphological and chemical compositional changes on biochar surfaces during the incubation in soil, scanning electron microscopy (SEM) with an energy dispersive spectrometer (EDS) was used. A JEOL JSM-6510LA EDS was operated at an accelerated voltage of 5 or 10 kV, which provided rapid, semi-quantitative analysis of the surface. Several regions and spots were investigated for each biochar.

2.4.6. XRD

X-ray diffraction (XRD) patterns of the soil (silt and clay) and pristine and recovered biochar samples were examined using a Rigaku SmartLab at 40 kV and 40 mA with a Cu-K alpha radiation source. Samples were dried, homogenized, and passed through a 0.05-mm sieve before preparing them for analysis on glass plates. A continuous 2θ scan mode from 15° to 70° was applied at a step size of 0.02 and scan speed of 1.5°/min. Observed XRD patterns were compared with standards compiled by Profex software (v 4.2.0) to identify crystalline phases.

2.4.7. Statistics

One-way analysis of variance (ANOVA) was conducted by Stata (version 12.0) to investigate the differences among the treatments. Significant differences were determined by the Tukey test at a 5% level, except for instances where specified. Correlation tests were also conducted where necessary.

3. Results

3.1. Physicochemical properties of the produced biochars

The characteristics of produced biochars are presented in Table 1. Generally, all the biochars had alkaline pH, except the JL biochar pyrolyzed at 300 °C (pH 6.36). Under the described pyrolysis conditions, the biochar yields ranged from 29.11% to 69.82%, with the highest for the CM300 biochar. As the pyrolysis temperature increased, biochar pH, ash content, and total P, K, Ca, and Mg content also increased. The total nitrogen content of the CM biochars was found to be substantially higher (10% and 4.69% for CM300 and CM500, respectively) than rest of the biochars. Besides, CM500 had the highest contents of ash, total P, and Ca among the biochars.. However, maximum K and Mg contents were found in dairy manure biochars. The carbon-to-nitrogen ratio (C/N) of the biochars had a very wide range (between 4.02 and 753), representing high variability in preserved nitrogen content.

3.2. Nitrogen release kinetics from the treatments

The results of the whole incubation period indicated that only the chicken manure-derived biochars were able to release significant amounts of nitrogen to satisfy the need for sweet corn. The addition of 2% CM300 and CM500 biochars made about 10.51 and 1.10 times more nitrogen available than the recommended fertilizer. On average, the recommended fertilizer dose is able to supply 76.40 mg-N/kg soil, whereas CM300 and CM500 treatments had available N of 803.5 and 84.3 mg/kg, respectively (Fig. 1a). In contrast, Japanese larch and dairy

Table 1
The physicochemical properties of produced biochars.

| Properties	Japanese Larch Biochar		Dairy Manure Biochar		Chicken Manure Biochar	
	300 °C	500 °C	300 °C	500 °C	300 °C	500 °C
pH	6.36	8.2	8.05	9.49	7.38	10.01
Yield (%)	52.66	29.11	55.66	41.07	69.82	47.98
Ash (%)	0.15	0.3	24.05	35.25	33.95	46.65
Volatile matter (%)	48.16	21.94	35.20	14.75	48.77	28.61
C (%)	67.77	83.25	52.56	54.06	40.19	35.98
N (%)	0.09	0.12	2.63	2.25	10.00	4.69
P (%)	0.07	0.11	1.03	1.20	1.63	2.09
K (%)	0.05	0.08	3.16	3.60	2.08	2.33
S (%)	ND	ND	0.35	0.30	0.53	0.61
Ca (%)	0.16	0.27	2.36	3.19	12.53	17.63
Mg (%)	0.03	0.04	1.08	1.38	0.87	1.07
C/N ratio	753.00	693.78	20.01	24.03	4.02	7.68

*ND = Not detected.
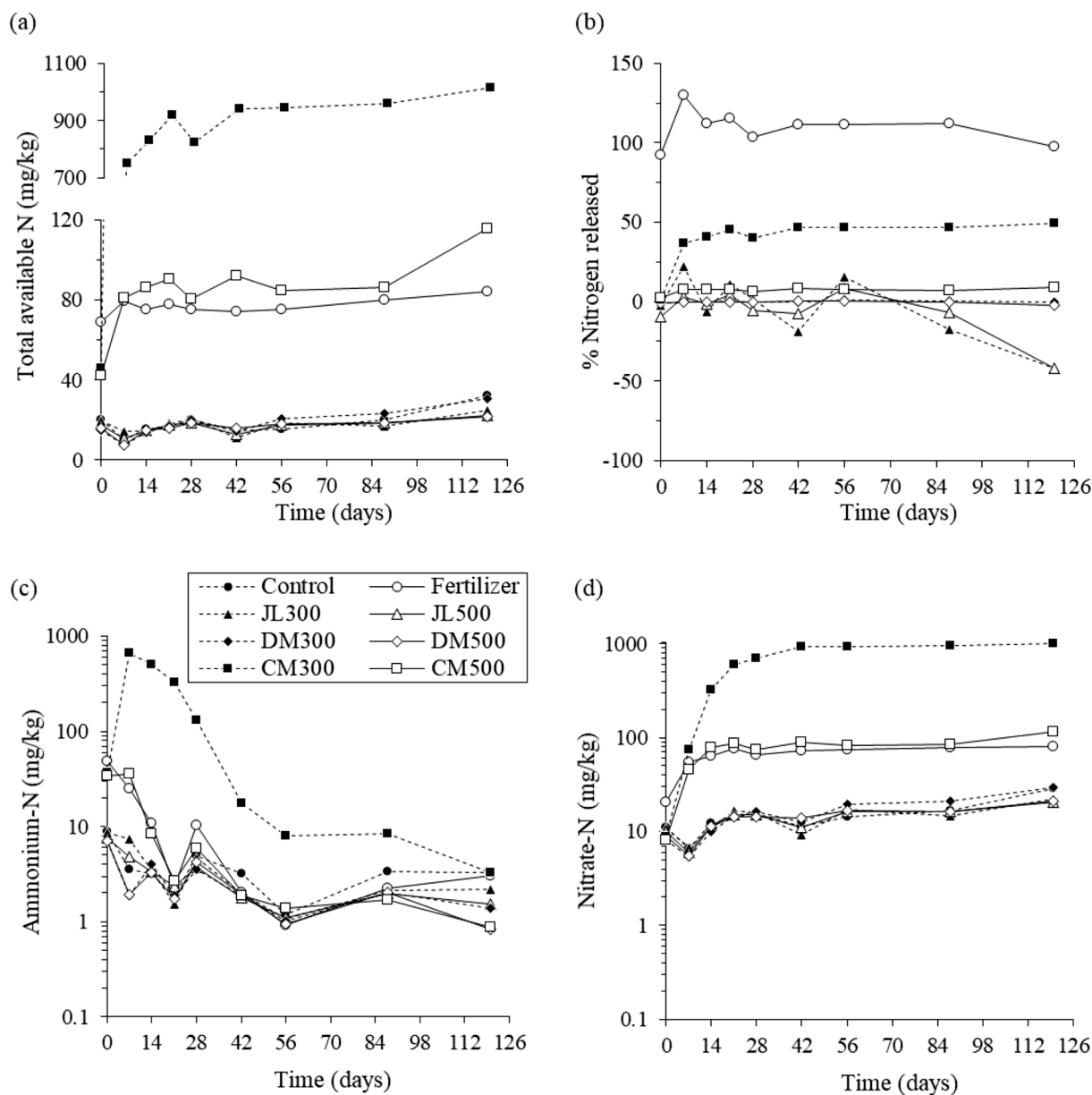
Fig. 1. Effect of fertilizer and biochar treatments on a) total nitrogen availability, b) % nitrogen released, c) ammonium-N, and d) nitrate-N.

manure biochar treatments had very little of the required available N. Application of these biochars reduced available nitrogen content on average, even compared to the control, and their production temperatures did not have any effect on N availability. The nitrogen release of manure-derived biochars was significantly correlated to the biochar-N content, and biochars with a C/N ratio of >20 could not increase available N in soil.

Regarding the release potential of N, release from chemical fertilizer was very rapid and reached its peak value (130%, more N became available than the applied treatment) within the first 7 days (Fig. 1b). This priming effect of N release from the soil itself was observed only in chemical fertilizer treatment. In contrast, CM300 treatment was able to release only 49% of its total N (120 days), the highest among the biochars, followed by CM500 (8.93%). The higher production temperature (500 °C) significantly reduced the nitrogen release in CM biochars. Fig. 1c shows that the release of ammonium-N peaked right after the introduction of fertilizer (0 days) and shortly after (7 days) for CM300 and CM500 treatments. The availability of ammonium-N decreased for chemical fertilizer treatment within 7 days, confirming a very fast

release and transformation. In contrast, a considerable amount of ammonium-N remained in CM300 treated soil up to 88 days (8.02 mg/kg), indicating its slow-release potential.

Generally, ammonium-N decreased with time and nitrate-N became the primary form of available N. Nitrate content followed a cumulative increasing trend, except for a little decrease at 28 or 42 days for some particular treatments (Fig. 1d). After the first 7 days of incubation, increasing NO_3^- content in CM biochar treatments was significantly ($p < 0.01$) correlated to decreasing NH_4^+, confirming subsequent nitrification of the released NH_4^-.

3.3. Influence of treatments on soil pH

Most of the treatments in this study reduced soil pH by the end of the incubation period. However, only the fertilizer and CM300 biochar significantly lowered the soil pH relative to the control, reducing it by 0.84 and 1.12 units, respectively (Fig. 2). The increasing nitrate content and soil pH of the treatments were found to be negatively correlated; however, it was only significant for CM300 at the 1% level.
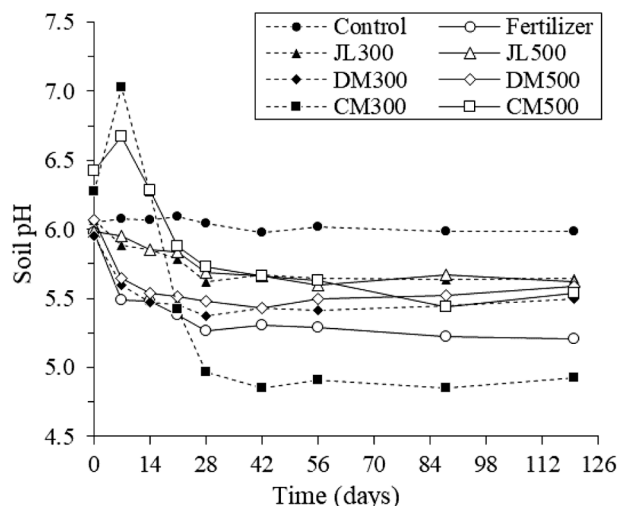
Fig. 2. Changes in soil pH after the application of biochars and recommended fertilizer.

Interestingly, both CM300 and CM500 biochar treatments caused an increase in soil pH (0.95 and 0.60 units, respectively) for the first seven days. However, after the first week, all treatments except the control exhibited a declining trend in soil pH.

3.4. Phosphorus release kinetics from the treatments

When biochar treatments were applied to the clay loam soil, all the manure-derived biochars released significantly ($p < 0.01$) more phosphorus than the recommended fertilizer dose (Fig. 3a). Available P (Mehlich-III) content in manure-derived biochar treatments ranged from 173 to 300 mg/kg (56–170% higher than the recommended dose of 111 mg/kg), and CM500 released the highest available-P, at 300 mg/kg, among the treatments. In contrast, Japanese larch biochar produced at both temperatures did not have a significant impact on the available phosphorus elevation in soil; rather it decreased it in most cases. If we consider the P release (%), CM500 was the most efficient with 47% of average release within 120 days, whereas synthetic fertilizer released only 12% of its P available for plants. Other manure-derived biochars such as DM500, CM300, and DM300 released 37%, 35%, and 35%,

respectively (Fig. 3b). Among all the biochar treatments, only the Japanese larch biochars showed a negative P release.

Fig. 3a shows a substantial P release by the treatments immediately after application. However, the large amount of available P soon declined. At 7 days of incubation, only the manure-derived biochars (except DM300) increased, but after 14 days, most of the treatments exhibited an increasing trend of P availability up to 28 days (Fig. 3a). On average, available P was 1.38 and 1.10 times greater in CM500 and DM500 treatments respectively than their low-temperature counterparts. Biochar produced at the higher temperature proved to be a significantly better treatment only for CM biochar.

Contrary to the expected increase in cumulative P availability, a portion of the initially released P in this study became unavailable over time (Fig. 3a). After 28 days of incubation, available P content started to decline only in the manure-derived biochar treatments, and later after 42 days, all the treatments illustrated a similar diminishing trend. The decline of P was more pronounced for high P-releasing manure biochar treatments. In particular, the CM500 biochar-treated soil had a major decline of available P (from 263 to 209 mg/kg) in the last 32 days.

3.5. Potassium release kinetics from the treatments

In terms of K availability in soil, manure-based biochar treatments had significantly ($p < 0.001$) higher available-K than all the other treatments (Fig. 4a). The K availability from manure-based treatments showed a fluctuating trend up to 42 days and followed a steadily declining pattern afterward. In general, both the DM and CM biochars produced at 500 °C statistically ($p < 0.05$) increased the maximum amount of available-K in soil. Both DM300 and CM300 biochar also released more K than the other treatments, and there was no significant difference between them. DM biochar (500 °C) provided the highest availability of K in soil (~1176 mg/kg); however, the highest average release (107–137%) was seen in CM biochars (Fig. 4b). It should be noted that the average K release exceeded 100% only in CM biochar treatments, which indicates additional K release from the soil itself. Biochar produced from Japanese larch showed no significant difference from the control in terms of K availability. After 42 days of incubation, almost all the treatments exhibited a declining trend in available K. Among the biochar treatments, the greatest reduction (278 mg/kg) in K availability occurred in the DM500 treatment within the last 78 days. By the end of the study, the CM500 biochar had the greatest available K, even more than DM500.
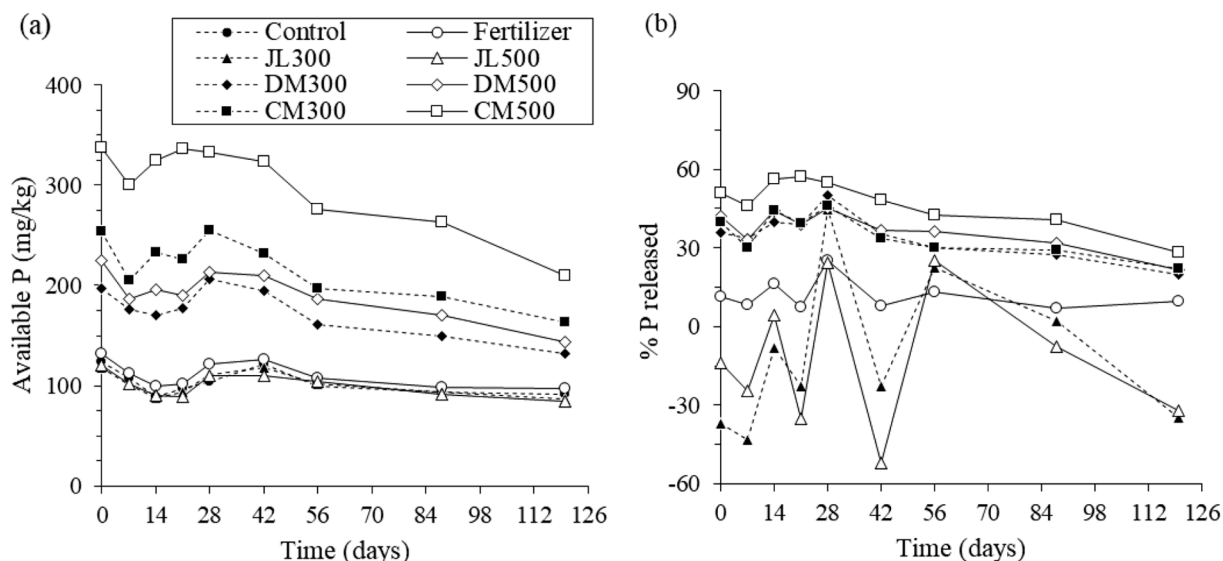

Fig. 3. Effect of fertilizer and biochar treatments on a) phosphorus availability and b) % phosphorus released.
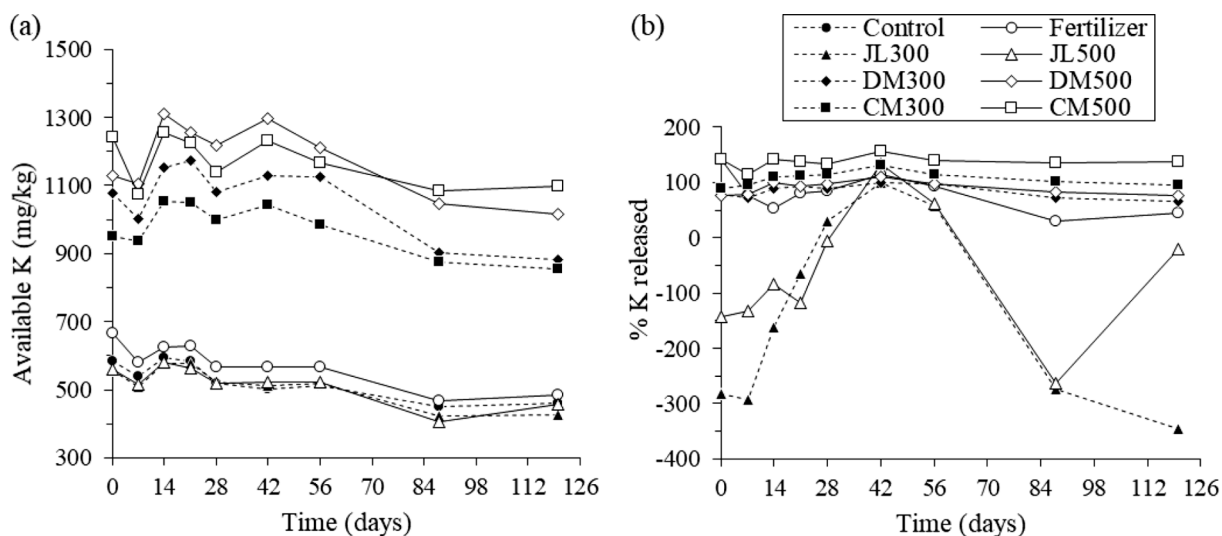
Fig. 4. Effect of fertilizer and biochar treatments on a) potassium availability and b) % potassium released.
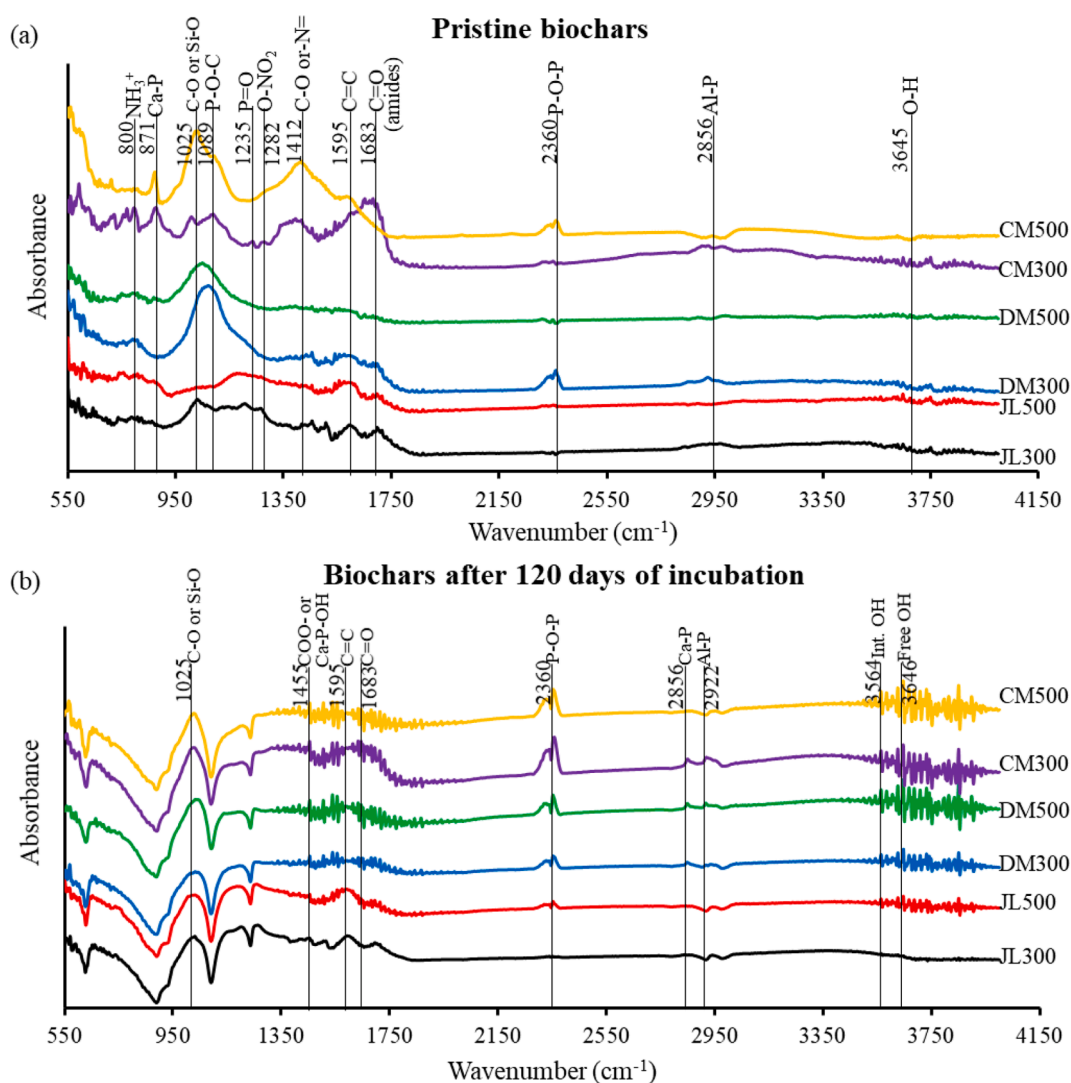

Fig. 5. FTIR-ATR spectra of pristine biochars (a), and biochars after 120 days of incubation (b). Major peaks of different functional groups are indicated.

3.6. Changes in biochar surface functional groups (FTIR analysis)

The ATR-FTIR spectra of the produced biochars showed many broad, overlapping peaks between 1700 and 600 cm^{-1} (Fig. 5a), indicative of the presence of both mineral and organic matter. The pristine biochars produced at 300 °C had greater absorbance than the biochars produced at 500 °C or biochars after incubation, which represented the disappearance of many functional groups with greater production temperature and during incubation. In biochars produced at 300 °C, a higher absorbance was seen between 1450 and 1600 cm^{-1} due to C = C bonds of aromatic compounds and the stretching of carboxylic groups (C=O, 1700–1740 cm^{-1}) compared to the same biochars produced at 500 °C. The most striking difference was seen for the CM biochar produced at 300 °C, which had a significantly broad peak of C=O at 1683 cm^{-1}, representing primary or secondary amides (Tipson, 1968). The broad peak had mostly disappeared in CM500, which indicates the condensation of aromatic structures with the increased temperature (Lawrinenko and Laird, 2015).

After biochars were incubated in soil, the peaks at 871 (Ca-P) and particularly the broad peak at 1683 cm^{-1} (amides) of the CM300 biochar gradually disappeared (Fig. 5b). These results confirm the dissolution of phosphates and nitrogenous amide compounds. In addition,

carbonate groups (1412 cm^{-1}) in CM biochars also declined with biochar incubation time. There was some noise in the FTIR patterns (Fig. 5b, at 1400–1800 cm^{-1} and 3500–3900 cm^{-1}), which might be attributed to rapid absorption of water vapor by the biochars during measurement.

3.7. Changes in biochar mineralogical composition

Overall, the produced biochars showed very little crystallinity, particularly for pristine JL biochars. The presence of calcite was significantly found in both CM biochars (Fig. 6a), which is consistent with the high Ca content found by chemical analysis (Table 1) and SEM-EDS. Together with numerous calcite minerals, there was evidence of magnesium phosphate, tetracalcium phosphate, hydroxyapatite, whitlockite, and sodium phosphate in CM biochars. The higher production temperature might have caused the abundance of phosphorus-dominant minerals in CM500 compared to CM300. Crystal phases of sylvite (KCl) were common in both DM biochars. There was also some evidence of diverse phosphate minerals (monopotassium phosphate, MPP; magnesium phosphate hydrate, Mg-P; and sodium dihydrogen phosphate, Na-P). Numerous unidentified peaks could represent inorganic phases retained in the C matrix of the biochars (Lawrinenko and Laird, 2015).

Fig. 6. XRD patterns of pristine biochars (a) and biochars after 120 days of incubation (b). Peaks of quartz (Qtz), calcite (Cal), sylvite (Syl), hydroxyapatite (Apt), monopotassium phosphate (MPP), magnesium phosphate hydrate (Mg-P), sodium dihydrogen phosphate (Na-P), tetracalcium phosphate (TCP), and whitlockite (Whi) minerals in XRD spectra are designated.

The XRD spectra after 120 days of incubation show that manure-derived biochars had increased orthophosphates on their surfaces (Fig. 6b). The whitlockite [$Ca_9(MgFe)(PO_4)_6PO_3OH$] peak at 28.4° 2θ in the CM500 biochar can be seen to disappear, indicating better dissolution of this mineral than apatite. Another significant change is the appearance of aluminum phosphate or aluminum phosphate hydrate peaks for almost all biochars. Sylvite (KCl), especially from DM500, can be seen to disappear, indicating significant dissolution of K.

3.8. Changes in biochar surface morphology and elemental composition (SEM-EDS)

The elemental compositions determined by EDS analysis in selected spots greatly differed from that of the whole surface area of the biochars. For example, the Ca, C, and O contents were 37.53%, 18.37%, and 44.10% in a spot of raw CM500 biochar representing $CaCO_3$, whereas for the entire surface they were 9.79%, 39.66%, and 18.88%, respectively (Figs. 7a, S1 and Table S3). After 120 days of incubation, clay-mineral complexes were seen on biochar surfaces. These complexes were characterized by a higher O:C ratio along with higher Si, Al, Ca, Mg, P, K, and Fe contents as measured by EDX (Table S1). In particular, Ca and P contents significantly increased on the surface of CM500 (19.31% and 10.25%, respectively). Al-Si-phosphate and Ca/Mg-Si-phosphate complexes were also seen to appear as P derivatives after 120 days of incubation, mainly on manure-derived biochars (Fig. 7b and Fig. S2). In contrast, most of the K on raw CM500 (13.49%) and DM500 (3.69%) disappeared (Table S3), indicating their higher dissolution potential.

3.9. Changes in biochar cation exchange capacity (CEC) and specific surface area (SSA)

Our results indicated that the aging of biochar in soil had a positive effect on increasing cation exchange capacity (CEC). The CEC of most of the biochars increased after the incubation period (120 days), except for CM biochars, which had a small decline after 60 days (Fig. 8a). The mean increase in CEC ranged from 99% for CM500 to 181% for JL500. Statistically ($p < 0.01$), the highest increase was recorded for DM300 as it gained an additional 55.78 cmol (+) kg^{-1} within 120 days of incubation. The increase in CEC of manure-based biochars was greater than the wood-based biochars. The CEC increase in low-temperature biochars was significantly ($p < 0.01$) higher than that in high temperature (500 °C) biochars.

The BET specific surface area (SSA) analysis of the raw biochars (Fig. 8b) illustrated that the higher production temperature increased SSA. The initial increase in SSA with production temperature ranged from 1.87 to 81.76 times that of their low-temperature counterparts. The highest SSA (168 m^2/g) was recorded in the high-temperature wood-based biochar (JL500). After incubation in the soil for 60 days, only the SSAs of DM500 and CM500 biochars increased significantly ($p < 0.05$). The enlargements of the SSAs were about 11 and 3 times more than the initial values for raw DM500 and CM500, respectively. No significant increase was seen in the JL500 biochar, though it gained 26.12 m^2 per gram. However, after 120 days of incubation, a small decline in SSA was seen in most of the biochars, except for CM500 and DM300. No significant correlation was found between nutrient availability and increased CEC or SSA.
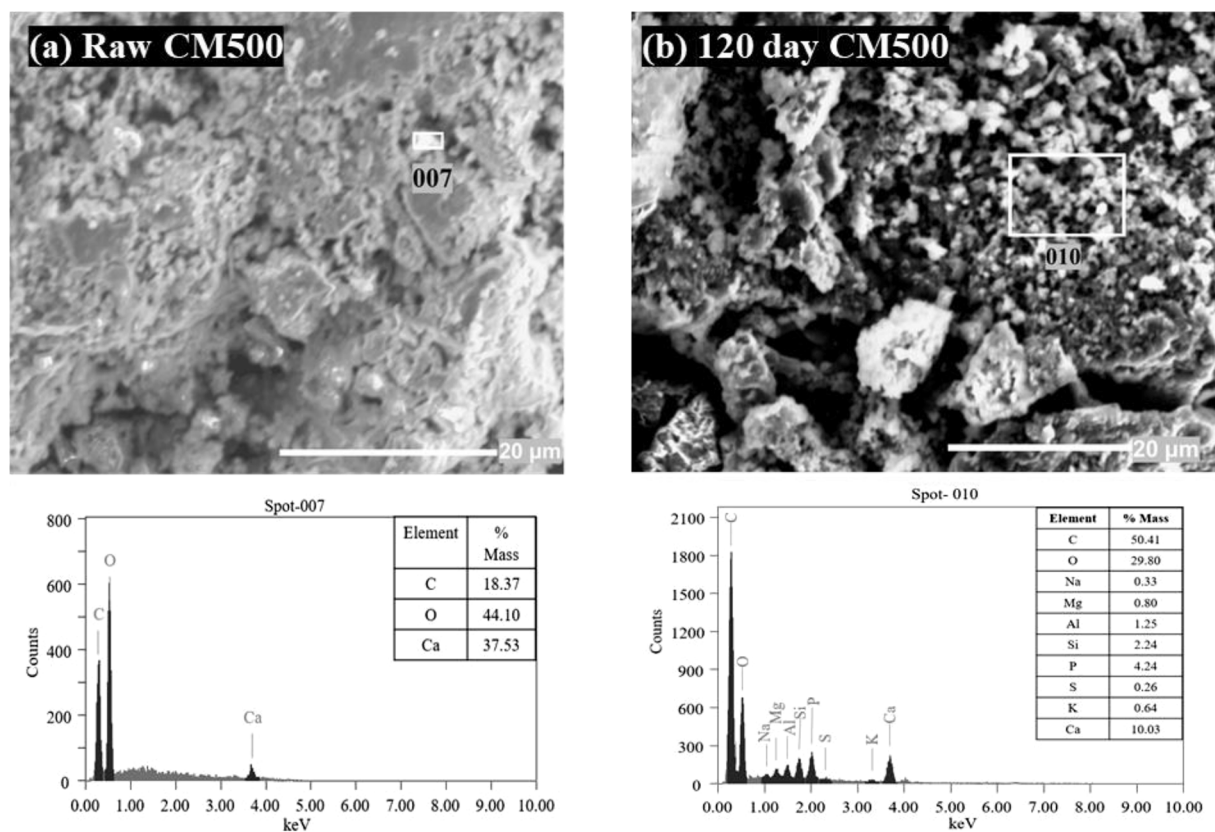

Fig. 7. Scanning electron micrographs (SEM) and associated energy dispersive X-ray spectroscopic (EDS) quantification of the CM500 biochar a) before and b) after 120 days of incubation.
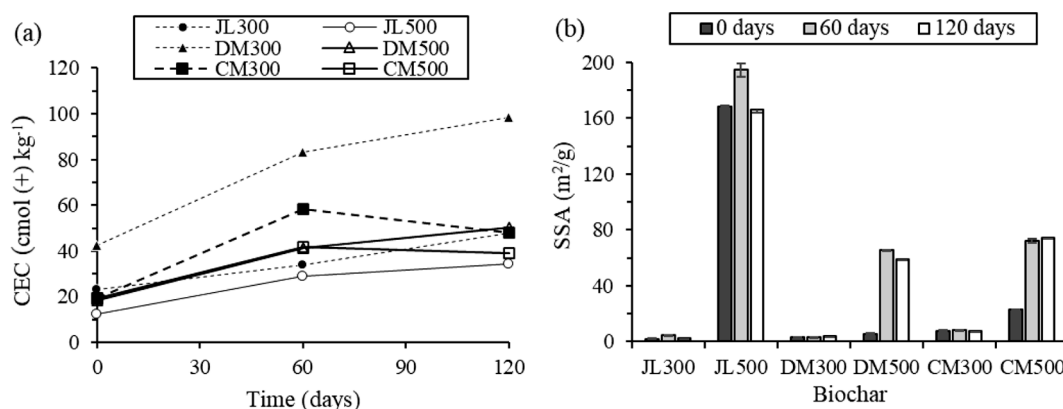
Fig. 8. Effect of incubation on biochar a) cation exchange capacity (CEC) and b) specific surface area (SSA).

4. Discussion

4.1. Biochar characteristics

The total nitrogen content of chicken manure biochars was substantially higher than that in previously reported (2.04 and 2.63%, respectively) literature (Sikder and Joardar, 2019; Wang et al., 2015), and pyrolysis at 300 °C preserved maximum N (10%). Recently, Ye et al. (2020) also suggested 300 °C pyrolysis for reduced gaseous N loss during production. Biochars produced at 500 °C lose significant N, which has previously been attributed to volatilization loss (as NH₃ mostly) from N-containing organic compounds (Cantrell et al., 2012; Clough et al., 2013). FTIR analysis in this study specifically revealed the decomposition of amides to be the underlying mechanism behind the reduced N content, especially from high N-containing feedstocks like CM. Additionally, with a very low C/N ratio (<8), CM biochar is expected to promote net mineralization (Chan and Xu, 2009) in soil. This can enhance the availability of nitrogen and other nutrients if the soil physicochemical conditions are optimal for microbial decomposition. However, unlike nitrogen, a higher production temperature (500 °C) increased the concentration of P and K in biochars with ash content.

4.2. Nitrogen release

Only the chicken manure biochars released enough nitrogen to satisfy the demand for sweet corn. Sikder and Joardar (2019) also confirmed significant plant growth and better N retention in clay loam soil by similar poultry litter biochar (300 °C). The relatively higher N and lower C/N ratio in chicken manure biochar might have stimulated N mineralization and release. The significant correlation between manure biochar N content and nitrogen release supports our hypothesis. However, immobilization of available nitrogen was also reported previously by poultry litter (~535 °C) biochar (Clark et al. 2019). Thus, finding a reasonable mechanism behind the high N release is essential to resolve these opposing claims. In this study, we found the dissolution of N-containing amides of the CM300 biochar to be the main mechanism behind the 49% N release, as amide dissolution and N release simultaneously occurred within the first 120 days (Fig. 5b and 1a). Amides can undergo many chemical reactions both in acidic and alkaline conditions. Acid-mediated hydrolysis might have occurred in this soil, which can release ammonium or nitrile compounds and ultimately form carboxylic groups (March and Smith, 2007). As a higher production temperature decomposes most of these amides, CM500 released comparatively very low N (8.93%), which was caused by lower N content and decreased mineralization. Physiosorption of N (mainly NO₃⁻) by CM500 can also contribute to the reduced N availability in this treatment (Gao et al., 2018).

These amide peaks were not seen in dairy manure feedstock, since

the ruminant digestive system of cows utilizes most protein and non-protein nitrogen and fibers (Fontenot and Jurubescu, 1980). Moreover, the low N content and high C/N ratio (above 20) of both JL and DM biochar might have stimulated N immobilization (Chan and Xu, 2009) and reduced N availability. This implies that biochar addition as a nitrogen source should be based upon the nitrogen content and C/N ratio. In contrast, the steady NH₄-N release pattern of CM300 biochar for a considerably long period (88 days) confirms its potential to satisfy N demand for the complete growth period. The excess available N in CM300 (Fig. 1a) can also be assimilated by microbes (Clough et al., 2013). However, Cheng and Wen (1997) claimed that the assimilated N can be slowly released again at the slow decomposition stage when rapid immobilization ceases. These two facts confirm the potential of CM300 biochar to act as a slow-release N fertilizer.

The enhanced nitrification of released ammonium explains the fact that biochar promotes nitrification in soil (Clough et al., 2013). Thies et al. (2015) suggested that the biochar-induced activation of ammonia-oxidizing archaea (AOA) and ammonia-oxidizing bacteria (AOB) is behind the nitrification process. Nitrification continues to occur even after significant pH reduction, which might be due to higher substrate availability (NH₄⁺) for the nitrifying process (Sahrawat, 2008). This extensive nitrification might cause substantial nitrate accumulation in soil, which is not desirable due to the inability of the soil to retain it. Subsequently, this nitrate-N might get lost by leaching or indirectly by providing a substrate for N₂O emission (Clough et al., 2013). Although CM biochars have proven to be an efficient substitute for chemical N fertilizer, tuning the production temperature, application rate and timing might enhance their efficiency further.

4.3. Reduction in soil pH

Alkaline biochars have been found to buffer soil acidity in most previous studies (El-Naggar et al., 2019) and there is often a positive correlation between biochar ash content and biochar pH. However, in this study, an overall reduction of soil pH was seen even though all manure biochars had high ash content. No significant correlation was found among biochar ash content, pH, and resulting soil pH. One possible reason behind the soil pH decline could be the relatively high amount of decomposable volatile matter (Table 1) in these low-temperature biochars. Microorganisms can easily decompose those small organic molecules and produce CO₂, organic acids, and ammonium ions and eventually reduce the pH. Additionally, a significant correlation between reduced soil pH and increased nitrate content in the CM300 treatment corroborates the fact that nitrification can reduce soil pH by releasing H⁺ ions. Zhao et al. (2014) also reported similar acidification of two subtropical soils by biochar application with additional N fertilizer. Lowering of the pH might cause more positive charges on biochar surfaces, which will ultimately reduce NH₃ volatilization and

enhance the adsorption of anions such as NO_3^- and $H_xPO_4^-$ (Mukherjee et al., 2011; Yin et al., 2017). However, in actual field conditions, changes in soil pH might not be the same. Because plants may uptake some portion of the released ammonium, additional H^+ can be released during ammonium uptake, and the magnitude of nitrification might be different as well.

4.4. Phosphorus release

We found that all the manure-derived biochar treatments significantly increased P availability in soil compared to the recommended fertilizer dose. One obvious reason is the substantial P input by manure-based biochars. However, previous studies have claimed that high P-containing biochar input does not always ensure better P availability. Gao et al. (2018), citing many previous studies, reported that biochar can reduce available P in soil by precipitation (mainly Ca-P) or ionic bonding. In this study, all manure biochars had a rapid P release initially, resulting from fast diffusion or desorption of orthophosphates when water was added to the treatments. After a slight decline within 7 days, the increasing trend of available P can be attributed to the slow and steady dissolution of $(Ca/Mg)_3(PO_4)_2$ minerals with the declining soil pH. The XRD analysis supported this by showing whitlockite $[Ca_{18}Mg_2(HPO_4)_2(PO_4)_{12}]$ dissolution and increased orthophosphates on biochar surfaces with incubation time (Fig. 6b). Wang et al. (2015) also found a comparable P increase in soil to be acid driven. The increased P availability and soil pH was negatively correlated, though not significantly. This lack of correlation can be attributed to released P being affected by other soil processes like fixation.

The higher production temperature of manure-derived biochars increased P availability in soil compared to their low-temperature counterparts. Greater phosphorus input and more favorable soil pH (close to neutral) are responsible for this increase. This implies that the production temperature of 500 °C is better than 300 °C for P availability from manure-derived biochars. In contrast, both Japanese larch biochars showed an overall negative P release. This result indicates that structurally bound P in wood biochar is hardly soluble. Moreover, soil phosphate might become unavailable by exchange reactions with oxygenated functional groups (Chintala et al., 2014).

The reduced availability of P in soil at the later stage of incubation indicates that a slow and steady P release rate of manure biochars might not always ensure constant P availability in the soil. Contrary to expectations, the initially released P in this study was fixed in the clay loam soil over time. After 28 days of incubation, when the declining trend of pH in most of the treatments stabilized, available P content started to decline, which could be explained by Al-caused fixation. According to Hashimoto et al. (2012), oxalate-extractable Al and Fe is highly correlated to the P retention capacity (PRC) in soils, and that Al has the single most important direct effect on PRC. XRD analysis of the recovered biochars showed existence of Al-phosphates on the surface. The SEM-EDS and FTIR analyses also revealed the coexistence of Al-phosphates and Ca-phosphates with the presence of Si and Mg. A similar process of P-fixation by Al/Fe/humus-P complex formation was previously reported by Wada and Gunjigake (1979) for soils in Kyushu and Hokkaido districts of Japan. It can thus be assumed that, with the cessation of pH-induced dissolution of Ca/Mg-phosphate minerals, P availability declined in the soil by aluminosilicate fixation. The remaining Ca/Mg-phosphates seen in EDS analysis were expected to be dissolved in the acidic soil. However, sandwiched incubation of biochars between nylon sheets might have reduced the soil-biochar interaction and restricted complete dissolution.

Even after significant fixation had occurred within 120 days, the manure-derived biochar treatments had 1.35 to 2.14 times more available P than the recommended fertilizer dose. These findings suggest that manure-based biochars have the potential to increase P availability in clay loam soil, probably for longer than one growing season. There was no significant correlation between the P release and coexisting NO_3^-,

Ca^{2+}, or Mg^{2+} concentrations in soil (Figs. 1d, S3 and S4). However, nitrification induced decline in soil pH, and the eventual P release suggests an indirect effect of other nutrients.

4.5. Potassium release

Our results indicated that the Mehlich-III-extractable K was released very rapidly from the manure-derived biochar treatments, which may have been due to the high solubility of K-containing salts (Angst and Sohi, 2013). Among those salts, the presence of sylvite (KCl) was identified by the XRD analysis, and much of that was dissolved within 120 days, especially from the DM500 biochar. This is in line with the highest K release from the DM500 treatment within a few days after application. Although XRD analysis could not reveal any particular mineral that caused the maximum release of K from CM biochars, SEM-EDS analysis confirmed a significant release by the reduction of surface K content on CM500 within 120 days of incubation (Table S1). Due to the quick releasing potential of K from biochars, it has been said to have a very short-term effect on soil (Angst and Sohi, 2013). After 42 days of incubation, a declining trend in available K was also observed. This can be attributed to K fixation into 2:1-type clay minerals in the soil (vermiculite for example). The K fixation was more prominent for DM biochar treatments, which may be due to having a lower co-existing Ca content. However, fixed K can be released further in the next crop growing season and is dependent on inherent soil chemical composition (Wang et al., 2018).

On the other hand, since the CM biochars were seen to exceed 100% release, they must have stimulated inherent K release from soil. This can be explained by two potential mechanisms. First, high Ca^{2+} content in the CM biochars might have released K by substitution reactions from clay particles. Limwikran et al. (2018) also reported significant K release by a $CaCO_3$-containing pineapple peel biochar. Second, released ammonium from CM biochars can also be fixed preferentially to potassium when added to clay-rich soil, releasing K^+ from the soil (Nielsen, 1972). There is evidence that both mechanisms increase K availability in the soil (Kolahchi and Jalali, 2007), although these relationships were not statistically proven in this study. Additionally, Wang et al. (2018) found that biochars can stimulate potassium-dissolving bacterial activity (that can solubilize K-bearing minerals and convert the insoluble K to soluble forms) in soil and increase plant uptake of K from soils that are abundant in 2:1-type K-bearing minerals (such as illite). By the end of this study, CM biochars showed the lowest fixation of K, which implies their potential to make K available for a considerable period of time.

4.6. Increase in CEC and BET specific surface area (SSA)

Incubation in soil increased the CEC of all the biochars. Biochar aging processes including abiotic and biotic oxidation of surface functional groups, loss of labile organic components, and sometimes sorption of microbially mediated organic matter onto biochar surfaces can increase CEC (Mukherjee et al., 2014). The CEC of manure-based or low-temperature biochars was comparatively greater than that of the wood or high-temperature biochars. El-Naggar et al. (2019), citing other literature, claimed that this could be due to high ash content in manures and by the oxidative aging of substantial surface functional groups. The increased CEC might have a positive effect on cationic nutrient (NH_4^+, K^+, Ca^{2+}) retention and availability, the reduction of exchangeable acidity, and NH_3 volatilization. However, the presence of some basic (e. g., amides, aromatic amines, and pyrimidinic) functional groups may allow biochars to retain anionic nutrients as well (Hollister et al., 2013).

The initial SSA was maximal in the wood-based JL500 biochar, which has previously been explained by the lower ash content of wood and the increased number of accessible micropores created after volatile components have been released by high production temperatures (Mukherjee et al., 2011). After incubation, the removal of ashes and tars from high ash-containing biochars (DM500 and CM500) to open up the

blocked pores might have caused a significant increase of SSA (Heitkötter and Marschner, 2015). Comparatively, a more porous surface was also seen during morphological analysis (SEM) of these biochars (Figs.7, S1 and S2). Therefore, the increased surface area and porosity might facilitate nutrient retention and a habitat for symbiotic microbes in the long run (Thies and Rillig, 2009).

The overall analysis of CEC and SSA proves that aging significantly increased the CEC of all biochars, whereas SSA was increased in only the manure-derived ones produced at 500 °C. This implies that aging-induced increases in biochar nutrient retention will mainly be governed by increased CEC rather than biochar SSA. Physiosorption might increase only in manure-based high temperature-produced biochars.

We are aware that the focus of this study was only on the overall availability of different nutrients and their release or transformation mechanisms. Biochar-stimulated nutrient release from the soil itself was not determined. However, the knowledge of a time-dependent interactive release mechanism provides a basis for future isotope-labeled nutrient dynamics studies from manure-derived biochars as a comprehensive nutrient source.

5. Conclusion

With the growing demand for animal protein, manure production has also substantially increased globally. Appropriate conversion of these manures into biochar and a better understanding of soil-specific nutrient release mechanisms can ensure safe recycling of these high-nutrient resources. Our results illustrated that chicken manure biochar produced at ≤500 °C can become a comprehensive source of N, P, and K for plants. A lower production temperature (300 °C) can yield manure biochars with significant nitrogen content with a slow-release potential, particularly from non-ruminant animals. High N-containing manure biochars can indirectly stimulate P dissolution by reducing soil pH. In contrast, a higher production temperature (500 °C) can increase the P and K release from both chicken and dairy manure biochars. Overall, this study has revealed the potential of manure-derived biochars for use as a comprehensive fertilizer or as a complementary amendment to the conventional chemical fertilizer. However, the 2% biochar application was excessive in some cases, requiring quantification of the soil-dependent optimum dose and residual agronomic value, preferably by field experiments.

Declaration of Competing Interest

The authors declare that they have no known competing financial interests or personal relationships that could have appeared to influence the work reported in this paper.

Appendix A. Supplementary data

Supplementary data to this article can be found online at https://doi.org/10.1016/j.geoderma.2021.115100.

References

Angst, T.E., Sohi, S.P., 2013. Establishing release dynamics for plant nutrients from biochar. GCB Bioenergy 5, 221–226.

Arden-Clarke, C., Hodges, R., 1988. The environmental effects of conventional and organic/biological farming systems. II. Soil ecology, soil fertility and nutrient cycles. Biol. Agric. Hortic. 5, 223–287.

ASTM D1762-84, 2013. Standard Test Method for Chemical Analysis of Wood Charcoal. ASTM International, Conshohocken, PA.

Cantrell, K.B., Hunt, P.G., Uchimiya, M., Novak, J.M., Ro, K.S., 2012. Impact of pyrolysis temperature and manure source on physicochemical characteristics of biochar. Bioresour. Technol. 107, 419–428.

Chan, K.Y., Xu, Z., 2009. Biochar: nutrient properties and their enhancement. Biochar Environ. Manag.: Sci. Technol. 1, 67–84.

Cheng, L.-L., Wen, Q.-X., 1997. Transformation and management of manure nitrogen. In: Nitrogen in Soils of China. Springer, pp. 281–302.

Chintala, R., Schumacher, T.E., McDonald, L.M., Clay, D.E., Malo, D.D., Papiernik, S.K., Clay, S.A., Julson, J.L., 2014. Phosphorus sorption and availability from biochars and soil/b iochar mixtures. CLEAN–Soil Air, Water 42, 626–634.

Clark, M., Hastings, M.G., Ryals, R., 2019. Soil carbon and nitrogen dynamics in two agricultural soils amended with manure-derived biochar. J. Environ. Qual. 48, 727–734.

Clough, T.J., Condron, L.M., Kammann, C., Müller, C., 2013. A review of biochar and soil nitrogen dynamics. Agronomy 3, 275–293.

Duku, M.H., Gu, S., Hagan, E.B., 2011. Biochar production potential in Ghana—a review. Renewable Sustainable Energy Rev. 15, 3539–3551.

El-Naggar, A., Lee, S.S., Rinklebe, J., Farooq, M., Song, H., Sarmah, A.K., Zimmerman, A. R., Ahmad, M., Shaheen, S.M., Ok, Y.S., 2019. Biochar application to low fertility soils: a review of current status, and future prospects. Geoderma 337, 536–554.

Fontenot, J., Jurubescu, V., 1980. Processing of animal waste by feeding to ruminants. In: Digestive Physiology and Metabolism in Ruminants. Springer, pp. 641–662.

Gao, S., DeLuca, T.H., Cleveland, C.C., 2018. Biochar additions alter phosphorus and nitrogen availability in agricultural ecosystems: a meta-analysis. Sci. Total Environ..

Guo, M., Uchimiya, S.M., He, Z., 2016. Agricultural and Environmental Applications of Biochar: Advances and Barriers. Soil Science Society of America.

Hashimoto, Y., Kang, J., Matsuyama, N., Saigusa, M., 2012. Path analysis of phosphorus retention capacity in allophanic and non-allophanic andisols. Soil Sci. Soc. Am. J. 76, 441–448.

Heitkötter, J., Marschner, B., 2015. Interactive effects of biochar ageing in soils related to feedstock, pyrolysis temperature, and historic charcoal production. Geoderma 245, 56–64.

Hokkaido Agriculture Department, 2015. Hokkaido fertilizer recommendations. Hokkaido Agriculture Department, Sapporo, Hokkaido, Japan.

Hokkaido Research Organization, 2012. Analytical method for soil and crop nutrition diagnosis. Hokkaido Research Organization, Sapporo, Hokkaido, Japan.

Hokkaido Research Organization, 2002. Sapporo city Agricultural land soil map. Hokkaido Research Organization, Sapporo, Hokkaido, Japan.

Hollister, C.C., Bisogni, J.J., Lehmann, J., 2013. Ammonium, nitrate, and phosphate sorption to and solute leaching from biochars prepared from corn stover (Zea mays L.) and oak wood (Quercus spp.). J. Environ. Qual. 42, 137–144.

Igalavithana, A.D., Ok, Y.S., Usman, A.R., Al-Wabel, M.I., Oleszczuk, P., Lee, S.S., 2016. The effects of biochar amendment on soil fertility. Agric. Environ. Appl. Biochar: Adv. Barriers 63, 123–144.

Ippolito, J.A., Spokas, K.A., Novak, J.M., Lentz, R.D., Cantrell, K.B., 2015. Biochar elemental composition and factors influencing nutrient retention. In: Biochar for Environmental Management: Science, Technology and Implementation, pp. 139–163.

Jones Jr., J.B., 2001. Laboratory Guide for Conducting Soil Tests and Plant Analysis. CRC Press.

Kamali, M., Jahaninafard, D., Mostafaie, A., Davarazar, M., Gomes, A.P.D., Tarelho, L., Dewil, R., Aminabhavi, T.M., 2020. Scientometric analysis and scientific trends on biochar application as soil amendment. Chem. Eng. J. 125128.

Kolahchi, Z., Jalali, M., 2007. Effect of water quality on the leaching of potassium from sandy soil. J. Arid Environ. 68, 624–639.

Lawrinenko, M., Laird, D.A., 2015. Anion exchange capacity of biochar. Green Chem. 17, 4628–4636.

Lehmann, J., Joseph, S., 2015. Biochar for Environmental Management: Science, Technology and Implementation. Routledge.

Lehmann, J., Rondon, M., 2006. Bio-char soil management on highly weathered soils in the humid tropics. Biol. Approach. Sustainable Soil Syst. 113, e530.

Limwikran, T., Kheorouenromne, I., Suddhiprakarn, A., Prakongkep, N., Gilkes, R., 2018. Dissolution of K, Ca, and P from biochar grains in tropical soils. Geoderma 312, 139–150.

March, J., Smith, M., 2007. March's Advanced Organic Chemistry: Reactions. Mechanisms and Structure. John and Wiley Sons Inc., New York.

Mukherjee, A., Zimmerman, A., Hamdan, R., Cooper, W., 2014. Physicochemical changes in pyrogenic organic matter (biochar) after 15 months of field aging. Solid Earth 5, 693.

Mukherjee, A., Zimmerman, A., Harris, W., 2011. Surface chemistry variations among a series of laboratory-produced biochars. Geoderma 163, 247–255.

Nielsen, J.D., 1972. Fixation and release of potassium and ammonium ions in Danish soils. Plant Soil 36, 71–88.

Ok, Y.S., Tsang, D.C., Bolan, N., Novak, J.M., 2018. Biochar from Biomass and Waste: Fundamentals and Applications. Elsevier.

Sahrawat, K., 2008. Factors affecting nitrification in soils. Commun. Soil Sci. Plant Anal. 39, 1436–1446.

Sikder, S., Joardar, J., 2019. Biochar production from poultry litter as management approach and effects on plant growth. Int. J. Recycl. Org. Waste Agric. 8, 47–58.

Song, W., Guo, M., 2012. Quality variations of poultry litter biochar generated at different pyrolysis temperatures. J. Anal. Appl. Pyrol. 94, 138–145.

Subedi, R., Taupe, N., Ikoyi, I., Bertora, C., Zavattaro, L., Schmalenberger, A., Leahy, J., Grignani, C., 2016. Chemically and biologically-mediated fertilizing value of manure-derived biochar. Sci. Total Environ. 550, 924–933.

Suliman, W., Harsh, J.B., Abu-Lail, N.I., Fortuna, A.-M., Dallmeyer, I., Garcia-Perez, M., 2016. Influence of feedstock source and pyrolysis temperature on biochar bulk and surface properties. Biomass Bioenergy 84, 37–48.

Sun, D., Hale, L., Kar, G., Soolanayakanahally, R., Adl, S., 2018a. Phosphorus recovery and reuse by pyrolysis: applications for agriculture and environment. Chemosphere 194, 682–691.

Sun, K., Qiu, M., Han, L., Jin, J., Wang, Z., Pan, Z., Xing, B., 2018b. Speciation of phosphorus in plant- and manure-derived biochars and its dissolution under various aqueous conditions. Sci. Total Environ. 634, 1300–1307. https://doi.org/10.1016/j.scitotenv.2018.04.099.

Thies, J.E., Rillig, M.C., 2009. Characteristics of biochar: biological properties. Biochar Environ. Manag.: Sci. Technol. 1, 85–105.

Thies, J.E., Rillig, M.C., Graber, E.R., 2015. Biochar effects on the abundance, activity and diversity of the soil biota. Biochar Environ. Manag.: Sci., Technol. Implementation 2, 327–389.

Tilman, D., Cassman, K.G., Matson, P.A., Naylor, R., Polasky, S., 2002. Agricultural sustainability and intensive production practices. Nature 418, 671–677.

Tipson, R.S., 1968. Infrared spectroscopy of carbohydrates.

Vitousek, P.M., Naylor, R., Crews, T., David, M., Drinkwater, L., Holland, E., Johnes, P., Katzenberger, J., Martinelli, L., Matson, P., 2009. Nutrient imbalances in agricultural development. Science 324, 1519–1520.

Wang, L., Xue, C., Nie, X., Liu, Y., Chen, F., 2018. Effects of biochar application on soil potassium dynamics and crop uptake. J. Plant Nutr. Soil Sci. 181, 635–643.

Wada, K., Gunjigake, N., 1979. Active aluminum and iron and phosphate adsorption in Ando soils. Soil Sci. 128, 331–336.

Wang, Y., Lin, Y., Chiu, P.C., Imhoff, P.T., Guo, M., 2015. Phosphorus release behaviors of poultry litter biochar as a soil amendment. Sci. Total Environ. 512–513, 454–463. https://doi.org/10.1016/j.scitotenv.2015.01.093.

Ye, Z., Liu, L., Tan, Z., Zhang, L., Huang, Q., 2020. Effects of pyrolysis conditions on migration and distribution of biochar nitrogen in the soil-plant-atmosphere system. Sci. Total Environ. 138006.

Yin, Q., Zhang, B., Wang, R., Zhao, Z., 2017. Biochar as an adsorbent for inorganic nitrogen and phosphorus removal from water: a review. Environ. Sci. Pollut. Res. 24, 26297–26309.

Zhao, X., Wang, S., Xing, G., 2014. Nitrification, acidification, and nitrogen leaching from subtropical cropland soils as affected by rice straw-based biochar: laboratory incubation and column leaching studies. J. Soils Sediments 14, 471–482.